# CW POSITRON SOURCE AT CEBAF

by

Serkan Golge
B.S. July 2002, Fatih University
M.S. December 2005, Old Dominion University

A Dissertation Submitted to the Faculty of
Old Dominion University in Partial Fulfillment of the
Requirement for the Degree of

DOCTOR OF PHILOSOPHY

PHYSICS

OLD DOMINION UNIVERSITY
July 2008

Approved by:

Charles E. Hyde (Director)

Arne Freyberger

Anatoly Radyuskhin

Moskov Amarian

Sacharia Albin

# ABSTRACT

# CW POSITRON SOURCE AT CEBAF

Serkan Golge
Old Dominion University, 2008
Director: Dr. Charles E. Hyde

Feasibilty of a CW positron source for the 6 GeV (and 12 GeV upgrade) recirculating linacs at Jefferson Lab is provided. The proposed 100nA CW positron source has several unique characteristics; high incident electron beam power (100kW),10 MeV/c incident electron beam momentum, CW incident beam and CW production. Positron production with 10 MeV/c electrons has several advantages; the energy is below neutron threshold activation so the production target and the optical system will not become activated during use; CEBAF requires a very low energy spread, so the absolute energy spread is bounded by the low incident energy. These advantages are offset by the large angular distribution of the outgoing positrons. Results of simulations of the positron production, capture and acceleration are presented. IAC test results and CEBAF admittance measurements are shown as well. Energy flow, power deposition and thermal management of the elements present a challenge and are included in the simulations.

# ACKNOWLEDGEMENTS

I would like to thank...

# TABLE OF CONTENTS

# LIST OF TABLES

Page

# LIST OF FIGURES

# CHAPTER I

# INTRODUCTION

# CHAPTER II

# PHYSICS WITH POSITRONS

## II.1 NUCLEAR PHYSICS

### II.1.1 Deeply Virtual Compton Scattering (DVCS)

### II.1.2 2-photon Annihiliation

### II.1.3 Dark Matter

## II.2 MATERIAL SCIENCE

# CHAPTER III

# POSITRON SOURCES

## III.1 WAYS TO CREATE POSITRONS

## III.2 PAST AND PRESENT SOURCES

## III.3 REVIEW OF ILC POSITRON SOURCE

# CHAPTER IV

# BASIC DESCRIPTION OF CEBAF

## IV.1 BEAM TRANSPORT TERMINOLOGY

## IV.2 INJECTOR

## IV.3 ARC

## IV.4 ADMITTANCE MEASUREMENT AT CEBAF

# CHAPTER V

# SIMULATION RESULTS

## V.1 SIMULATION OF PAIR PRODUCTION

### V.1.1 Benchmarking with Theory

## V.2 OPTIMIZATION

## V.3 DESIGN OF LATTICE

### V.3.1 Genetic Algorithm

### V.3.2 DIMAD and OPTIM schematics

# CHAPTER VI

# IAC TEST RESULTS

## VI.1 PROFILE

Target thickness optimization is an important process to get the highest yield. Fig. 1 and Fig. 2 show conversion target thickness vs. conversion efficiency of positrons for different incoming elecron beam energies. It can be seen from Fig. 1 that 10 MeV electron beam yield peaks around 1.25 mm ($L_0 = 0.36X_0$ ) of tungsten thickness.

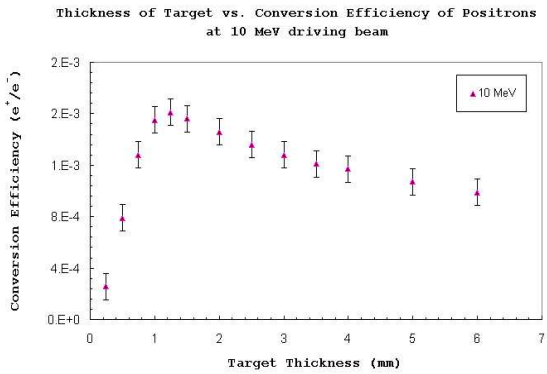


FIG. 1: Changing tungsten thickness vs the yield of positrons per electron at 10 MeV incoming electron beam.

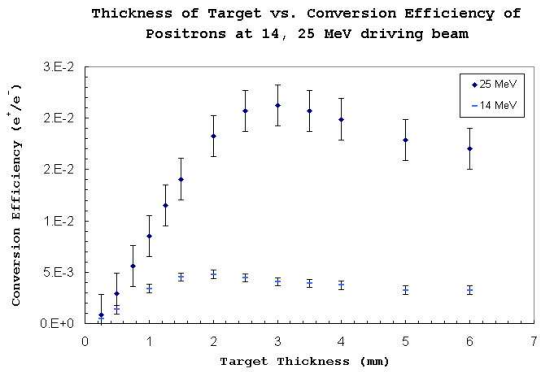


FIG. 2: Changing tungsten thickness vs the yield of positrons per electron at 14 and 25 MeV incoming electron beams.

In the simulation the driving electron beam is; $P(e^-)$ =10 MeV/c±5%, $\sigma_{xy}$ =3mm. Fig. 3(a) shows the momentum distribution of emitted positrons from tungsten, and $X - X'$ phase space is shown in Fig. 3(b).

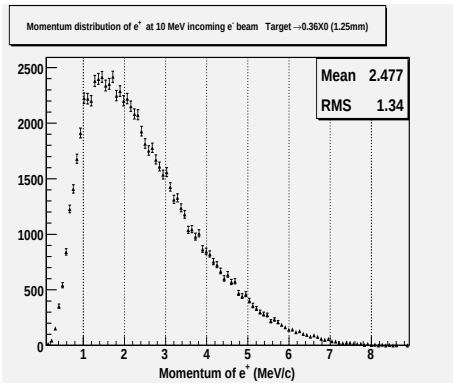


(a) Momentum Distribution.

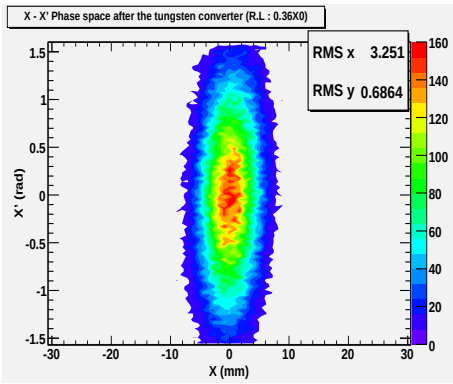


(b) $X - X'$ phase space.

FIG. 3: Momentum and Phase space distribution of positrons right after tungsten.

Fig. 4 we see the momentum vs. opening angle of positrons. Here opening angle(X*′*) is defined as the following:

$$x' = \arctan \frac{p_x}{p_z}. \tag{1}$$

where $P_x$ and $P_z$ are momentum components of positrons.

While it is clearly seen that momentum peaks around 2 MeV, within the desired emittance space 3 MeV positrons give us much yield. Fig. 5 shows momentum bins vs the yield of positrons for different emittances. For example; 2 represents positron momentums between; 1.75 MeV/c $\leq P(e^+) \leq$2.25 MeV/c.

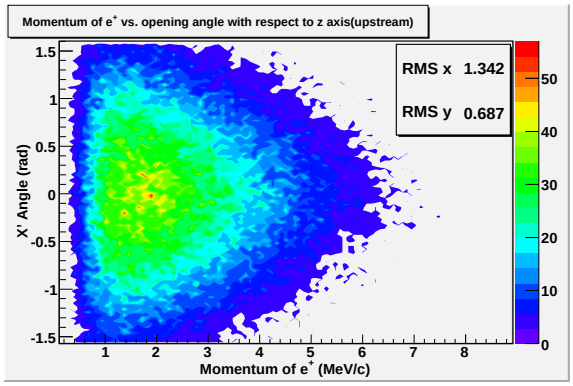


FIG. 4: Momentum vs. opening angle of positrons. Incoming electron beam is 10 MeV/c

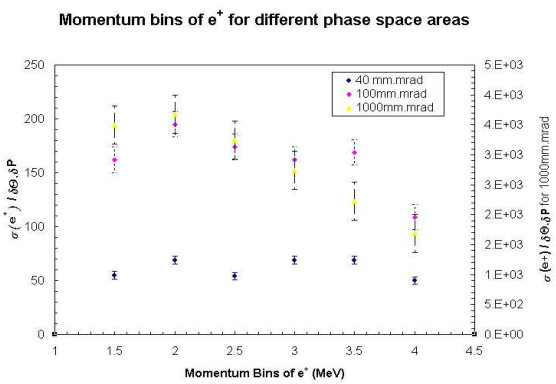


FIG. 5: Momentum bins vs the yield of positrons for ensembles of 40, 100 and 1000 mm.mrad transverse phase spaces.

## VI.2 DESIGN

The need for confirming our simulation results and ability to prepare a big scale project led us to do a preliminary measurement at Idaho Accelerator Center (IAC). First and most suitable design for our expextations is the following design: A quadrupole triplet selects tunable certain momentum band of positrons and dumps the off momentum positrons and electrons which is positioned right after the converter, another triplet prepares twiss parameters for the bends, a dipole-quad-dipole achromat design seperates positrons from electrons. Achromatic design supresses the huge mometum dispersion as well. It is sketched out in Fig. 6

The lattice design including evolution of the twiss-beta function is shown in Fig. 7.

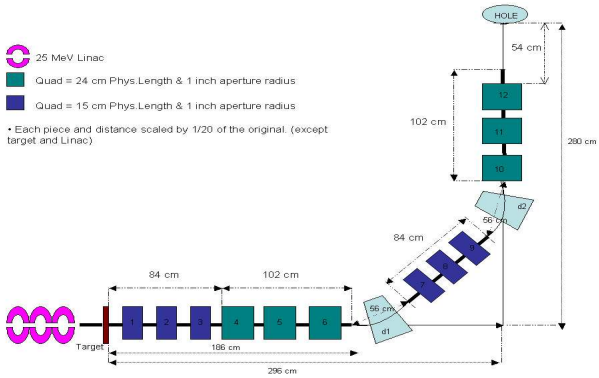


FIG. 6: IAC tunable positron design including an achomatic lattice

The beta function nicely evolves without comprimising the global lattice limit($\sigma_{xy} \leq \frac{d}{2}$ to get % 95 transportation).

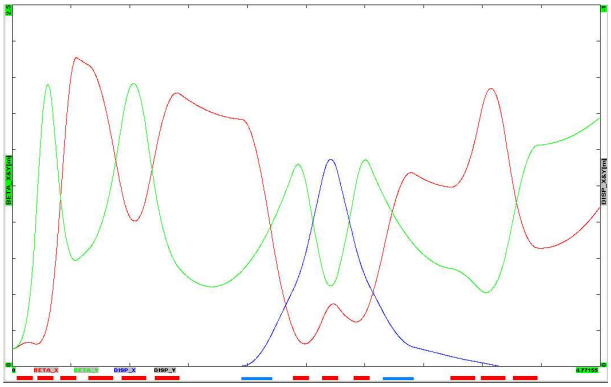

FIG. 7: IAC design Optim file showing the evolution of $\beta_{xy}$, and $D_{xy}$ functions.

In this proposed design, we will have the opportunity to tune the positron beam with desired momentum spread; dump off-momentum electrons and positrons at first stage; seperate the remaining electrons (the ones with the same momentum band of $e^+$) ; suppress the dispersion with the dipole-quad-dipole achomatic lattice; and finally transport noise free beam to the detector area.

Another design(let's call 'Green Run'), with a doublet positioned right after the converter tungsten, we will not be able to control the beam as we wanted, and dispersion will continue to grow rapidly leading all the off-momentum positrons scraped off . A schematic is shown in Fig. 8.

The optim twiss-beta evolution graph is shown in Fig. 9. As it can be seen in the graphs, dispersion can not be supressed with this configuration.

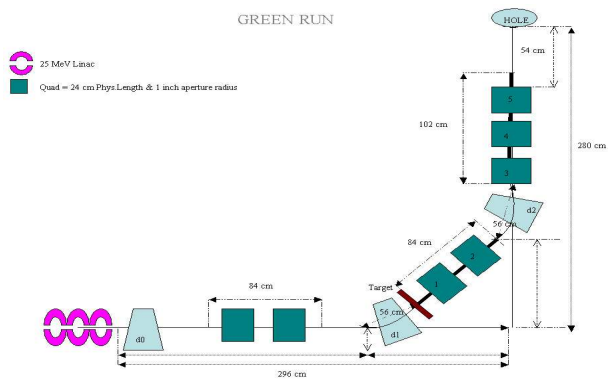


FIG. 8: IAC Green Run lattice schematic.

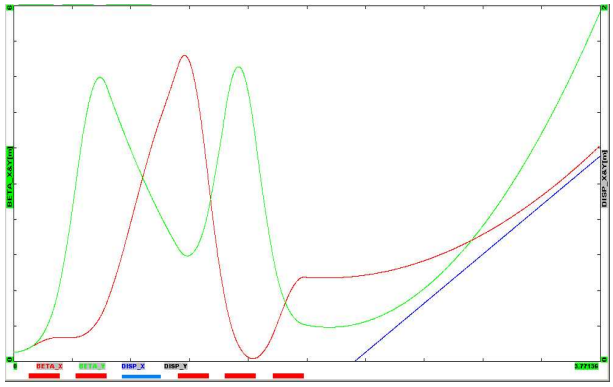


FIG. 9: IAC Green Run beta-evolution through the lattice. The blue curve is the dispersion.

A G4Beamline schematic is shown in Fig. 10. Here yellow cylinders are Q3 Type quads at IAC. Red figures are $45^0$ bends; purple is the beam pipe and lead block is shown in brown and white long cylinder is the accelerator section.

Simulation shows a beam profile of positrons at the detector as shown in Fig. 11.

With our first optimal configuration the conversion efficiency $\frac{e^+}{e^-} = 40x10^{-8}$, while in the 'green run' we have $10^{-8}$ which is 40X less.

The last configuration option is shown in Fig. 12. This configuration proposes an alternative beam line parallel to the primary 25 MeV beam line, with a $90^0$ bend to steer positrons into the detector hall. This option is not more advantegous than the Green Run, since a $90^0$ bend is not sufficient alone to supress the dispersion.

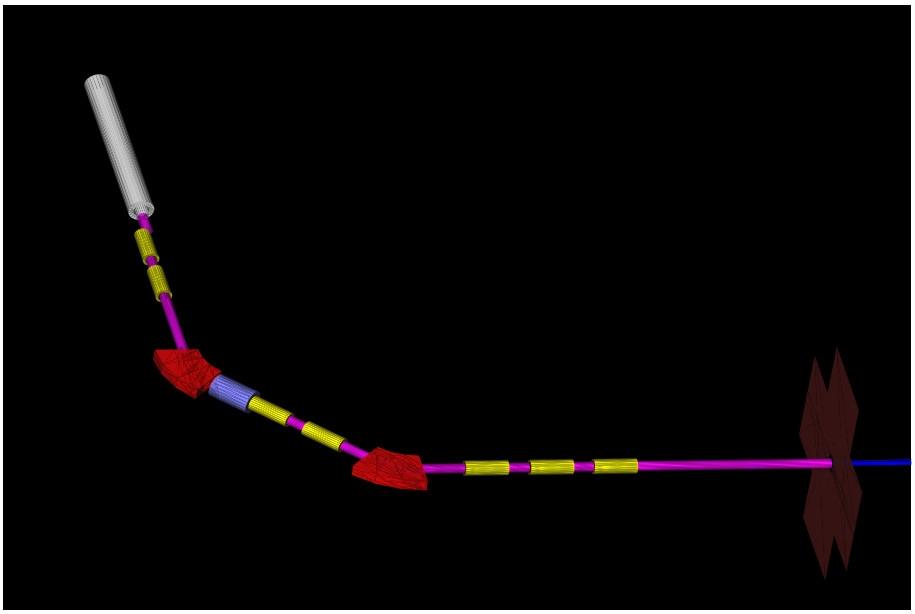

FIG. 10: Green Run G4Beamline snapshot.

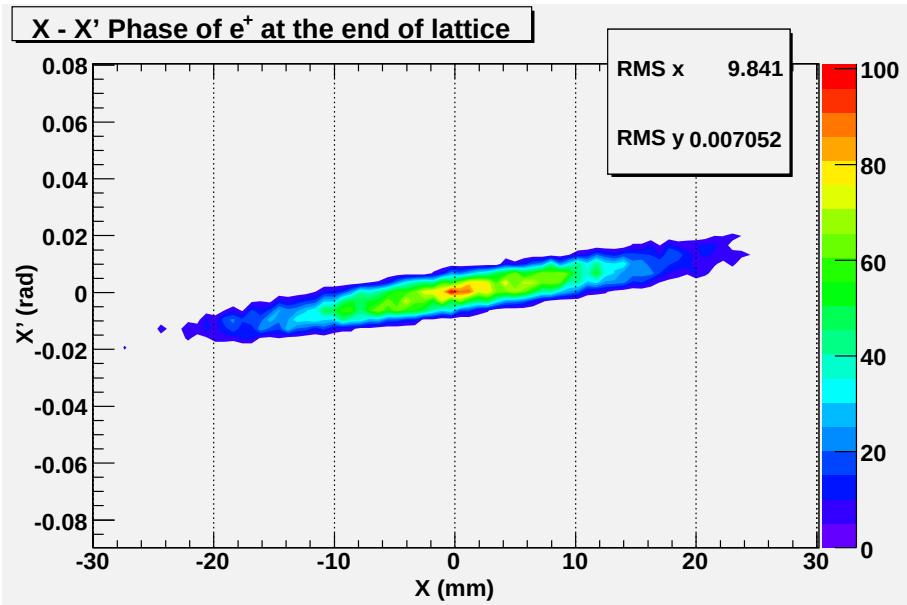


FIG. 11: $X - X'$ phase space of positrons at the detector located in the hole.

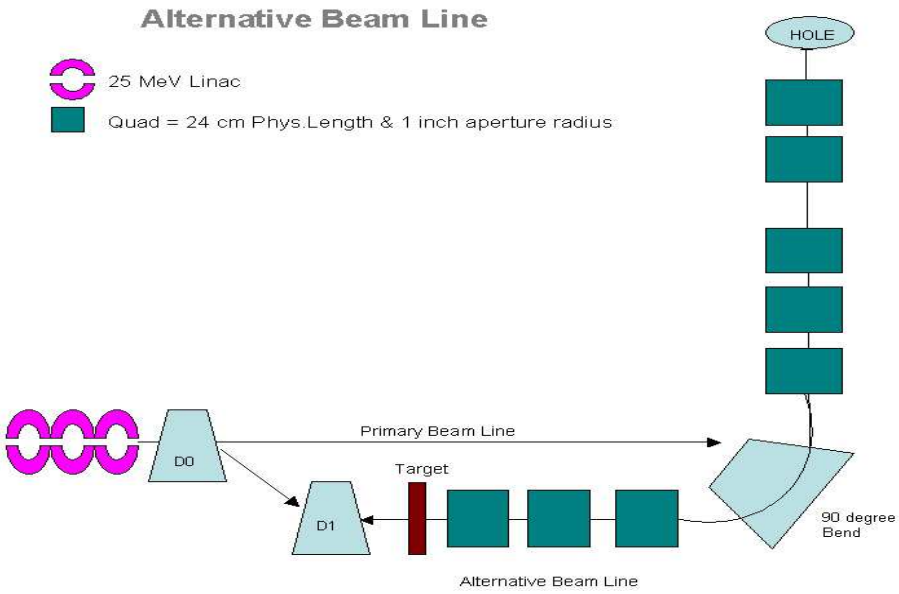


FIG. 12: Alternative Beam line.